

See discussions, stats, and author profiles for this publication at: <https://www.researchgate.net/publication/38052557>

Charge Transport and Dipolar Relaxations in Imidazolium-Based Ionic Liquids

ARTICLE *in* THE JOURNAL OF PHYSICAL CHEMISTRY B · OCTOBER 2009

Impact Factor: 3.3 · DOI: 10.1021/jp908519u · Source: PubMed

CITATIONS

38

READS

33

4 AUTHORS, INCLUDING:



Friedrich Kremer

University of Leipzig

302 PUBLICATIONS 6,177 CITATIONS

SEE PROFILE

Charge Transport and Dipolar Relaxations in Imidazolium-Based Ionic Liquids

C. Krause, J. R. Sangoro,* C. Iacob, and F. Kremer

Institute of Experimental Physics I, University of Leipzig, Linnéstrasse 5, 04103, Leipzig, Germany

Received: September 3, 2009; Revised Manuscript Received: October 1, 2009

Charge transport and dipolar relaxations in a series of imidazolium-based ionic liquids are studied by means of broadband dielectric spectroscopy. Despite the shift of more than 5 decades in the dielectric spectra upon systematic variation of the anion, scaling with respect to the dc conductivities and the characteristic rates yields a collapsing plot. The dielectric spectra are described at higher frequencies in terms of dipolar relaxations whereas hopping conduction in a random spatially varying energy landscape is quantitatively shown to dominate the spectra at lower frequencies. The β -relaxations observed for both the precursor and the ionic liquids are assigned to librational motion of the imidazolium ring. The corresponding dielectric strength exhibits a strong dependence on the anion.

Introduction

Ionic liquids are promising for manifold technological as well as fundamental applications because they exhibit unique features such as low-melting points, low-vapor pressures, wide liquid ranges, high-thermal stability, high conductivity, and wide electrochemical windows.^{1–5} The quest for quantitative understanding of charge transport in these materials is necessitated by the dire need for more efficient and optimal power sources among others. In addition, since ILs are also typically good glass-formers, they offer a rare opportunity to address basic questions regarding the correlation between ion conduction and the dynamic glass transition in the broadest length- and time-scales as well as localized molecular fluctuations (secondary relaxations). Because of its ability to measure the complex dielectric function (and hence the complex conductivity) over many orders of magnitude in frequency and in a wide temperature interval, broadband dielectric spectroscopy turns out to be an ideal experimental tool for this pursuit.⁶

Charge transport in ionic liquids is an active topic of current research.⁷ In recent studies of a series of ionic liquids, scaling of the complex dielectric function respectively the complex conductivity function with respect to quantities describing charge transport namely the characteristic rate ω_c respectively the dc-conductivity σ_0 at different temperatures has been shown to deliver collapsing plots. On the basis of combined dielectric and dynamic mechanical spectroscopy measurements, it was also established that the characteristic charge transport rate ω_c in ionic liquids is comparable to the structural α -relaxation rate ω_α .⁸ However, systematic study of the composition dependence on the static dielectric parameters such as the dielectric strength as well as localized ion dynamics such as β -relaxations and the inter-relationship thereof remains unexplored. In addition, the influence of these quantities on charge transport in ionic liquids have not been investigated.

Secondary relaxations at frequencies higher than those of the main structural α -process are observed in many glass formers. These processes can often be accounted for by the motion of a molecular side group in a polymer. While investigating super-cooled rigid molecules a few decades ago, Johari and Goldstein detected β -relaxations although intramolecular motion were not

expected of such materials at the time. So they proposed that the process is a property of the glassy state, a conjecture that is still under discussion.⁹ Recently, Rivera and Rössler elucidated the existence of β -processes in a series of room temperature ionic liquids which they attributed to a common butyl group.¹⁰ The question regarding the origin and nature of secondary relaxations is far from answered and ILs have ushered in new twists in the debate. For instance, the role played by neighboring ions in the local ion dynamics and a possible link to glassy dynamics as well as charge transport remains unclear.

In this article, it is demonstrated via novel scaling approach that the charge transport mechanisms in a series of ionic liquids based on the 1-hexyl-3-methylimidazolium cation are identical despite huge variations in transport quantities such as dc conductivities. The temperature dependence of the dielectric strength corresponding to charge transport is also investigated. Furthermore, secondary relaxations in the materials probed are shown to be dominated by contributions from the imidazolium ring. The anions are found to strongly influence the dielectric strength of the β -relaxations.

Experimental Section

The series of ionic liquids investigated in this study (1-hexyl-3-methylimidazolium tetrafluoroborate, [HMIM][BF₄], molecular weight = 254 g mol⁻¹; 1-hexyl-3-methylimidazolium bromide, [HMIM][Br], molecular weight = 247.18 g mol⁻¹; 1-hexyl-3-methylimidazolium chloride, [HMIM][Cl], molecular weight = 202.73 g mol⁻¹; 1-hexyl-3-methylimidazolium iodide, [HMIM][I], molecular weight = 294.18 g mol⁻¹; 1-hexyl-3-methylimidazolium hexafluorophosphate, [HMIM][PF₆], molecular weight = 312.24 g mol⁻¹; purity >98%) based on the same 1-hexyl-3-methylimidazolium cation as well as the precursor liquid, namely, 1-hexyl-2-methylimidazole (molecular weight = 166.26 g mol⁻¹, purity >98%) were purchased from Iolitec GmbH. The materials were used as received. The dielectric measurements in the frequency range (0.1 Hz to 10 MHz) and temperature interval (114–350 K) were carried out by means of a Novocontrol high resolution alpha dielectric analyzer. The analyzer was supported by Quatro temperature controller using pure nitrogen as heating agent and providing a temperature stability better than 0.2 K. Electric field in the range between 3 and 6 Vcm⁻¹ was applied for all materials. The measurements

* To whom correspondence should be addressed.

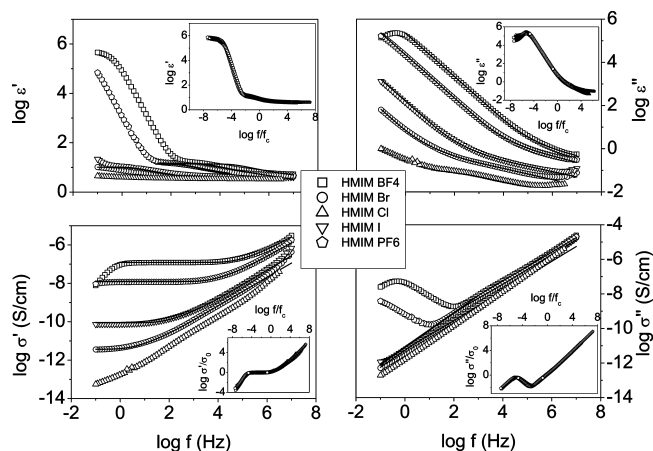


Figure 1. Complex dielectric function ($\epsilon^*(\omega) = \epsilon'(\omega) - i\epsilon''(\omega)$) and complex conductivity function ($\sigma^*(\omega) = \sigma'(\omega) + i\sigma''(\omega)$) of different ionic liquids based on the same 1-hexyl-3-methylimidazolium cation at $T = 220$ K. Inset: Scaling with respect to the characteristic frequency ω_c and dc conductivity σ_0 of the different ionic liquids. Lines denote fits by the random barrier model proposed by Dyre given in eq 1 ([HMIM][BF₄], $\tau_c = 9.58 \times 10^{-6}$ s, $\sigma_0 = 1.22 \times 10^{-7}$ S cm⁻¹; [HMIM][Br], $\tau_c = 0.17$ s, $\sigma_0 = 3.69 \times 10^{-12}$ S cm⁻¹; [HMIM][Cl] (out of spectral range); [HMIM][I], $\tau_c = 0.01$ s, $\sigma_0 = 8.83 \times 10^{-7}$ S cm⁻¹; [HMIM][PF₆], $\tau_c = 9.00 \times 10^{-5}$ s, $\sigma_0 = 1.23 \times 10^{-8}$ S cm⁻¹). The error bars are smaller than the size of the symbols, if not explicitly indicated otherwise. The logarithm is to base 10.

were conducted using stainless steel electrodes in parallel plate capacitor configuration.

Results and Discussion

The complex dielectric function, $\epsilon^*(\omega, T)$ is equivalent to the complex conductivity function, $\sigma^*(\omega, T)$ expressed as $\sigma^* = i\omega\epsilon_0\epsilon^*$ where $\epsilon^*(\omega) = \epsilon'(\omega) - i\epsilon''(\omega)$ and $\sigma^*(\omega) = \sigma'(\omega) + i\sigma''(\omega)$ where ϵ_0 is the permittivity of vacuum. It should be pointed out that the two formalisms emphasize different facets of the underlying mechanisms. Thus, both representations should be used to enhance clarity.

The conductivity σ' is characterized on the low frequency side by the plateau value of which directly yields the dc conductivity, σ_0 , and the characteristic radial frequency, ω_c , at which dispersion sets in and turns into a power law at higher frequencies. On the other hand, the real part of the dielectric function ϵ' at $f_c = (\omega_c/2\pi)$ turns from the high frequency limit to the static value ϵ_s . At lower frequencies, it is observed that σ' decreases from σ_0 and this is due to electrode polarization that results from blocking of charge carriers at the electrodes.¹¹

Figure 1 presents the dielectric spectra of different ionic liquids all based on the same 1-hexyl-3-methylimidazolium cation at $T = 220$ K. Systematically varying the anion while keeping the cation constant results in significant differences in the charge transport quantities (i.e., σ_0 varies from [HMIM][BF₄] to [HMIM][Br] over 5 decades). Via scaling with respect to σ_0 and ω_c it is remarkable that a coinciding plot is obtained as shown in the inset of Figure 1. This implies an identical underlying mechanism of charge transport in all ionic liquids investigated in this study.^{8,12} On the log–log plot of ϵ' versus frequency, it is observed that the dielectric strength does not seem to change significantly with the anion. This is investigated in further detail by the random barrier model (solved within the continuous-time random walk approximation) proposed by Dyre to describe the dielectric strength corresponding to charge transport. According to this model, charge transport in disordered systems is due to hopping of charge carriers in spatially varying

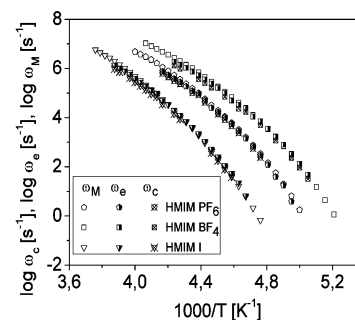


Figure 2. Activation plot for different characteristic electrical rates ω_c (as obtained from σ'), ω_M (as obtained from the maximum in $M''(\omega)$) and ω_e as taken from the fit using eq 1 for different ionic liquids as indicated. The error bars are smaller than the size of the symbols, if not explicitly stated otherwise. The logarithm is to base 10.

random energy landscape.^{13,14} The time corresponding to the attempt rate to overcome the highest barrier determining the dc conductivity, σ_0 , is one of the characteristic parameters of the model and is denoted by τ_c . The model approximates the complex dielectric function by the analytical equation

$$\epsilon^*(\omega) = \epsilon_\infty + \frac{\sigma_0\tau_c}{\epsilon_0(\ln(1 + i\omega\tau_c))} \quad (1)$$

where ϵ_∞ is the relaxed value of ϵ' . As shown in Figure 1, eq 1 yields a quantitative fit to the experimental data. It is however inapplicable at very low frequencies where electrode polarization effects show up since these are not accounted for in the model. This is discussed in detail elsewhere.¹¹ At higher frequencies, slight deviations that become more pronounced at lower temperatures are observed. These are due to secondary relaxations discussed later in this article.

One of the two key parameters describing charge transport according to eq 1 is ω_c . The equivalence of frequency of the peak in the imaginary part of the complex modulus (defined from $\epsilon^* = 1/M^*$, where $M^* = M' + iM''$; M' and M'' are the real and imaginary parts, respectively) M'' and the characteristic frequency ω_c at which the real part of conductivity σ' begins to increase with increasing frequency for disordered ion conducting solids has been pointed out by a number of researchers.^{6,13} In Figure 2, these three rates are compared for different ionic liquids. The remarkable coincidence obtained indicates that ω_c , ω_e , and ω_M in ionic liquids describe an identical underlying process, that is, electrical relaxation.

In Figure 3, a plot of σ_0 versus ω_c is presented. The Barton–Nakajima–Namikawa (BNN) relation,^{15–17} as this similarity is often described, has been shown to be a direct result of a combination of Einstein, Einstein–Smoluchowski, and Maxwell relations. On the basis of the quantitative agreement between ω_c and the structural α -relaxation rate as measured by dynamic mechanical spectroscopy, it has been concluded that glassy dynamics enhance charge transport in ionic liquids.⁸ It should be pointed out that the quantitative scaling underscores the weak composition dependence of the static parameters such as the dielectric strength (corresponding to the charge transport) and the static dielectric permittivity in a log–log representation for the ILs studied.

The precursor of the ILs (i.e., 1-hexyl-2-methylimidazole whose chemical structure is shown in the inset c of Figure 3) is investigated to gain further insight into the link between charge transport, and glassy dynamics as well as secondary relaxations. Imidazole consists of three carbon atoms and two nitrogen atoms

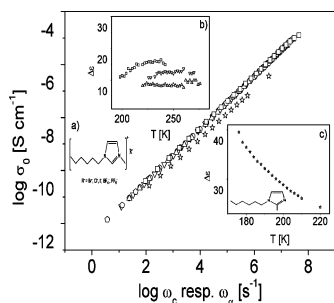


Figure 3. dc-conductivity σ_0 versus the structural α -relaxation rates ω_α of 1-hexyl-2-methylimidazole respectively the characteristic rates of charge transport ω_c for the different ionic liquids. Inset: (a) chemical structure of the different imidazolium-based ionic liquids; (b) dielectric strength versus temperature for [HMIM][BF₄] (open squares), [HMIM][Cl] (open triangles), and [HMIM][I] (inverted open triangles). An approximation based on the random barrier model proposed by Dyre given by eq 1 was used to fit the dielectric spectra yielding values for the dielectric strength; and (c) the dielectric strength corresponding to the structural α -relaxation versus $\log \omega_\alpha$ for 1-hexyl-2-methylimidazole (inset: its chemical structure) ([HMIM][Br] (open triangles), [HMIM][PF₆] (open pentagons), 1-hexyl-2-methylimidazole (open stars)). The error bars are smaller than the size of the symbols, if not explicitly indicated otherwise. The logarithm is to base 10.

at nonadjacent positions forming the diunsaturated imidazolium ring, which has a strong dipole moment of 3.84 Debyes while the hexyl-group is nonpolar.¹⁸ Whereas the BNN plot of ILs yields a collapsing plot, an analogous representation for the precursor liquid shows a systematic deviation as presented in Figure 3. This is explained by taking into account the dielectric strength and its temperature dependence. On the basis of the equivalence of the complex conductivity and dielectric functions, one expects a direct relationship between the measured static properties (such as the dielectric strength) and the dynamic quantities such as the charge transport and structural relaxation rates. It turns out that the dielectric strength of 1-hexyl-2-methylimidazole exhibits a stronger temperature dependence as compared to the ILs (see inset b and c of Figure 3) and increases with decreasing temperature as is usual for glass formers. However, it remains practically constant over the measured temperature range for all ILs (inset b of Figure 3). The systematic divergence observed in the BNN plot of precursor liquid with respect to the ILs may thus be possibly attributed to the different temperature dependence of their respective dielectric strengths.

To compare charge transport and structural α -relaxation, the characteristic rates are plotted for the different liquids as displayed in Figure 4. The temperature dependence of charge transport quantities is approximated by Vogel–Fulcher–Tammann equation expressed as

$$v(T) = \frac{1}{2\pi\tau(T)} = v_\infty \exp\left[\frac{-DT_0}{T - T_0}\right] \quad (2)$$

where $v_\infty = (2\pi\tau_\infty)^{-1}$, D is a constant, and T_0 is the Vogel-temperature (sometimes referred to as the ideal glass transition temperature). It is observed that the differences in the rates (ω_c , ω_α) and σ_0 (see inset of Figure 4) become more pronounced as the liquids are cooled down to the calorimetric glass transition temperature, T_g (whose experimental time scale is conventionally defined as 100 s). The fit parameters obtained using eq 2 are shown in Table 1a,b. As expected, the values of T_0 from the VFT-fits follow a similar sequence as those of the experimentally determined T_g .

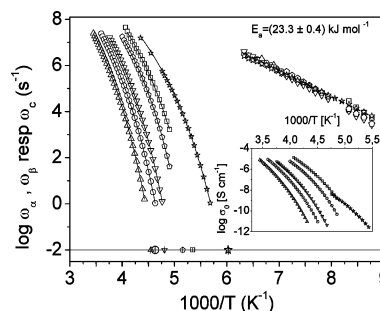


Figure 4. Temperature dependence of the structural α -relaxation rates of 1-hexyl-2-methylimidazole and the characteristic rates of charge transport as well as β -relaxations for the different ionic liquids. The full lines are fits made by Vogel–Fulcher–Tammann equation (eq 2) whereas the dashed lines are fits by eq 4 to the experimental data. Inset: dc conductivity σ_0 as a function of inverse temperature ([HMIM][BF₄] (open squares), $T_g = 187$ K; [HMIM][Br] (open circles), $T_g = 216$ K; [HMIM][Cl] (open triangles), $T_g = 220$ K; [HMIM][I] (inverted open triangles), $T_g = 208$ K; [HMIM][PF₆] (open pentagons), $T_g = 194$ K; 1-hexyl-2-methylimidazole (open stars), $T_g = 166$ K). The error bars are smaller than the size of the symbols, if not specified otherwise. The experimentally determined values of calorimetric glass transition temperature T_g are indicated by open symbols with vertical line.

Additional secondary processes are observed in these liquids at higher frequencies and lower temperatures. The β -relaxations are fitted by means of the empirical Havriliak–Negami function

$$\varepsilon^* = \varepsilon_\infty + \frac{\Delta\varepsilon}{(1 + (i\omega\tau_{HN})^\beta)^\gamma} \quad (3)$$

where ε_∞ is the relaxed value of ε' , τ_{HN} is the Havriliak–Negami relaxation time, and β , γ are shape parameters indicating the symmetric respectively asymmetric broadening of the complex dielectric function, the values of which are given in Table 2. The molecular relaxation rates are related to the characteristic time obtained from eq 2 by $\omega_{\max} = (1/\tau_{HN})[\sin(\beta\pi)/(2 + 2\gamma)]^{1/\beta}[\sin(\beta\gamma\pi)/(2 + 2\gamma)]^{-1/\beta}$. As presented in Figure 4, the β -relaxation shows an Arrhenius-type temperature dependence, described by

$$\log \omega_\beta(T) = \log \omega_\infty - \frac{\ln 10 E_A}{k_B T} \quad (4)$$

where E_A is the activation energy, ω_β is the relaxation rate of the process, k_B is the Boltzmann constant, and ω_∞ is the relaxation rate in the high temperature limit. In contrast to ω_c and ω_α , a single coinciding plot is obtained for ω_β . Because of the fact that all ionic liquids are based on the same cation, the beta-relaxation is certainly reminiscent of the contribution of the cation. Since the relaxation rates of 1-hexyl-2-methylimidazole coincide with the ω_β values obtained for ILs, it is concluded that β -relaxation is due to libration motion of the imidazolium ring. The activation energy for the secondary process as calculated by means of the fit to Arrhenius equation (eq 4) is (23.3 ± 0.4) kJ mol⁻¹. This value is comparable to those obtained by Rivera and Rössler for a different series of imidazolium based ionic liquids and fits well into the picture of localized molecular fluctuations.¹⁰

To estimate the influence of the anion on the β -relaxation process the imaginary part of the complex dielectric function ε'' as a function of scaled frequency is compared for the different ionic liquids and 1-hexyl-2-methylimidazole as shown in Figure

TABLE 1: Fit Parameters Obtained by Applying the VFT-Equation (Equation 2)^a

(a) Characteristic Rates of Charge Transport in the Various Ionic Liquids As Well As the Structural α -Relaxation Rates of 1-Hexyl-2-methylimidazole			
ionic liquid	$\omega_{\text{inf}} [\text{s}^{-1}] \pm 0.4 \text{ E13}$	$T_0 [\text{K}] \pm 2 \text{ K}$	$D \pm 1.0$
[HMIM][BF4]	2.4×10^{13}	147	3.9
[HMIM][Br]	6.2×10^{13}	161	4.6
[HMIM][Cl]	1.5×10^{14}	165	5.1
[HMIM][I]	4.5×10^{13}	159	4.3
[HMIM][PF6]	1.4×10^{13}	155	3.6
1-hexyl-2-methylimidazole	9.4×10^{12}	133	3.8

(b) dc-Conductivity σ_0 of the Various Ionic Liquids and the Precursor Liquid			
ionic liquid	$\sigma_{\text{inf}} [\text{S/cm}]$	$T_0 [\text{K}] \pm 2 \text{ K}$	$D \pm 1.0$
[HMIM][BF4]	4.1 ± 0.5	149	3.5
[HMIM][Br]	25.1 ± 1.12	161	4.7
[HMIM][Cl]	64.7 ± 4.2	164	5.3
[HMIM][I]	8.9 ± 0.6	161	4.1
[HMIM][PF6]	2.0 ± 0.2	158	3.3
1-hexyl-2-methylimidazole	$6.2 \times 10^{-2} \pm 6.5 \times 10^{-3}$	138	3.1

^a The pre-exponential factor is renamed in accordance with the quantity under study.

TABLE 2: Shape Parameters β and γ Derived by Employing the Havriliak–Negami Equation (Equation 3) to the Dielectric Spectra Corresponding to the β -Relaxations for the Different Ionic Liquids and 1-Hexyl-2-methylimidazole

ionic liquid	$\beta \pm 0.1$	$\gamma \pm 0.1$
[HMIM][BF4]	0.4	0.2
[HMIM][Br]	0.6	0.4
[HMIM][Cl]	0.7	0.3
[HMIM][I]	0.7	0.4
[HMIM][PF6]	0.7	0.3
1-hexyl-2-methylimidazole	0.5	0.4

5. It is surprising that despite the coinciding relaxation rates, there are considerable differences (about two decades between [HMIM][BF4] and its precursor) in the absolute values of ϵ'' . The normalized spectra of ϵ'' reveals no additional broadening with respect to variation of the anion as evident in the inset of Figure 5. The dielectric strength is nearly temperature independent (see inset b of Figure 5) but exhibits a pronounced dependence on the anion. This difference between the ionic liquids can be qualitatively explained by the Kirkwood–Fröhlich–Onsager approach that describes the dielectric strength as $\Delta\epsilon = [(1/(3\epsilon_0))Fg[\mu^2/(k_B T)]n]$, where $\Delta\epsilon$ is the dielectric strength, ϵ_0 is the permittivity constant, μ^2 is the mean square dipole moment for noninteracting isolated dipoles, F is the

Onsager factor, $g = 1 + [\langle \sum_{i=1}^N \sum_{j=1}^N \mu_i \mu_j \rangle] / (\bar{N} \mu^2)$ the Kirkwood–Fröhlich correlation factor to model the interaction between the dipoles, k_B is the Boltzmann factor, T is the temperature, and $n = (N/V)$ the number density.^{19,20} Since [HMIM][BF4] has comparably high number density ($n = 2.72 \times 10^{27} \text{ m}^{-3}$), it exhibits the highest dielectric strength. For the number density of [HMIM][PF6] a slightly lower value ($n = 2.50 \times 10^{27} \text{ m}^{-3}$) is obtained as for the maximum of the peak. This description seems to work well for ionic liquids based on the two spherically shaped anions ([BF4] and [PF6]) also known to be less interacting. The ion–ion interaction in halides is extensively studied and follows the order $\text{I}^- < \text{Br}^- < \text{Cl}^-$ thereby explaining the experimentally observed sequence.²¹

In conclusion, the dielectric spectra of ionic liquids is shown to be quantitatively described by the random energy barrier model. Whereas the characteristic charge transport rate and dc conductivity vary over 6 decades with temperature, the corresponding dielectric strength is practically temperature independent. This underscores the fact that the static dielectric permittivity, a quantity that is of direct benefit in understanding solvation dynamics, and electrical double layers among others, exhibits only a weak dependence on the anion and is practically temperature independent within the range studied. Detailed analysis reveals that secondary relaxation processes are dominated by librations of the imidazole/imidazolium ring. No broadening of the β -relaxation peak is observed upon variation of the anion.

Acknowledgment. Financial support from the Deutsche Forschungsgemeinschaft under the DFG SPP 1191 Priority Program on Ionic Liquids is gratefully acknowledged.

References and Notes

- (1) Welton, T. *Chem. Rev.* **1999**, 99, 2071.
- (2) Schulz, P. S.; Müller, N.; Bösmann, A.; Wasserscheid, P. *Angew. Chem., Int. Ed.* **2007**, 46, 1293.
- (3) (a) Kornyshev, A. A. *J. Phys. Chem. B* **2007**, 111, 5545. (b) Turton, D. A.; Hunger, J.; Stoppa, A.; Heftner, G.; Thoman, A.; Walther, M.; Buchner, R.; Wynne, K. *J. Am. Chem. Soc.* **2009**, 131, 11140–11146. (c) Sangoro, J. R.; Jacob, C.; Serghei, A.; Naumov, S.; Galvosas, P.; Kärger, J.; Wespe, C.; Bordusa, F.; Stoppa, A.; Hunger, J.; Buchner, R.; Kremer, F. *J. Chem. Phys.* **2008**, 128, 212509.
- (4) Fernicola, A.; Scrosati, B.; Ohno, H. *Ionics* **2006**, 12, 95.
- (5) Earle, M. J.; Seddon, K. R. *Pure Appl. Chem.* **2000**, 72, 1391.
- (6) Kremer, F.; Schönhals, A. *Broadband Dielectric Spectroscopy*; Springer: Berlin, 2003.

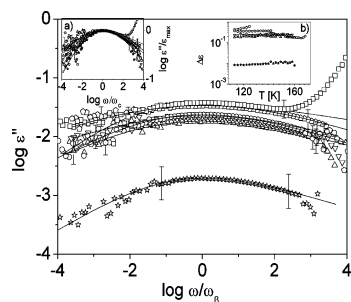


Figure 5. Scaled spectra of the imaginary part of complex dielectric function with respect to the β -relaxation rate ω_β . Inset: (a) $\epsilon''/\epsilon''_{\text{max}}$ versus scaled frequency, and (b) the temperature dependence of the dielectric strength $\Delta\epsilon$ for the different materials under study ([HMIM][BF4] (open squares), [HMIM][Br] (open circles), [HMIM][Cl] (open triangles), [HMIM][I] (inverted open triangles), [HMIM][PF6] (open pentagons), 1-hexyl-2-methylimidazole (open stars)).

- (7) Dorfmueller, T.; Williams, G. *Molecular Dynamics and Relaxation Phenomena in Glasses*; Springer: Berlin, 1987.
- (8) Sangoro, J. R.; Iacob, C.; Serghei, A.; Friedrich, C.; Kremer, F. *Phys. Chem. Chem. Phys.* **2009**, *11*, 913–916.
- (9) Johari, G. P.; Goldstein, M. *J. Chem. Phys.* **1970**, *53*, 372.
- (10) Rivera, A.; Rössler, E. A. *Phys. Rev. B* **2006**, *73*, 212201.
- (11) (a) Sangoro, J. R.; Serghei, A.; Naumov, S.; Galvosas, P.; Kärger, J.; Wespe, C.; Bordusa, F.; Kremer, F. *Phys. Rev. E* **2008**, *77*, 051202. (b) Klein, R. J.; Zhang, S.; Dou, S.; Jones, B. H.; Colby, R. H.; Runt, J. *J. Chem. Phys.* **2006**, *124*, 144903. (c) Serghei, A.; Tress, M.; Sangoro, J. R.; Kremer, F. Electrode polarisation and charge transport at solid interfaces. *Phys. Rev. B*, accepted for publication, **2009**.
- (12) (a) Roling, B.; Happe, A.; Funke, K.; Ingram, M. D. *Phys. Rev. Lett.* **1997**, *78*, 2160. (b) Sidebottom, D. L. *Phys. Rev. Lett.* **1999**, *82*, 3653. (c) Zielniok, D.; Eckert, H.; Cramer, C. *Phys. Rev. Lett.* **2008**, *100*, 035901.
- (13) Dyre, J. C. *J. Phys. C: Solid State Phys.* **1986**, *19*, 5655.
- (14) Dyre, J. C. *J. Appl. Phys.* **1988**, *64*, 5.
- (15) Barton, J. L. *Verres Refract.* **1966**, *20*, 328.
- (16) Nakajima, T. *Annual Report, Conference on Electric Insulation and Dielectric Phenomena*; National Academy of Sciences: Washington DC, 1971.
- (17) Namikawa, H. *J. Non-Cryst. Solids* **1975**, *18*, 173.
- (18) Hamano, H.; Hamaka, H. F. *Tetrahedron* **1962**, *18*, 985–990.
- (19) Böttcher, C. J. F. *Theory of electric polarization. Dielectric in static fields*; Elsevier: Amsterdam, 1973; Vol. 1.
- (20) Fröhlich, H. *Theory of Dielectrics*; Oxford University Press: London, 1958.
- (21) Zhuo, K.; Liu, H.; Tang, J.; Yujuan, C.; Wang, J. J. *Phys. Chem. B* [Online early release]. DOI:10.1021/jp904477w.

JP908519U